Donor-Site-Acceptor Dual-Modulation Covalent Organic Frameworks for Synergistic U(VI) Photoreduction and Immobilization

Xin Zhong [a, b, *], Zhehong Ji

[a] School of Life and Environmental Sciences, Shaoxing University, Huancheng West Road 508, Shaoxing 312000, P.R. China

[b] Zhejiang Key Laboratory of Functional Ionic Membrane Materials and Technology for Hydrogen Production, Shaoxing 312000, P.R. China

Xin Zhong: zhongxinmagic@163.com

1. Photocatalysis experiments

The performance of U(VI) photoreduction was studied by using TpPa-N_x (x=0,1,2,3) materials as photocatalysts and carried out in air, and Xenon lamp with 420 nm cut-off filter as the light source. Parallel experiments were carried out in multiple double-layer jacketed quartz reactors equipped with cooling water circulation system (CEL-LAB500, China Education Au-light). Specifically, 2.0~6.0 mg of COFs was added to 33 mL U(VI) solution (25~70 mg/L, pH 4.0~6.0, containing 3 mL methanol), then stirred vigorously in the dark for 120 min to achieve adsorption equilibrium before triggering the photocatalytic reaction. Afterwards, regularly extract 1 ml of solution to determine the residual U(VI) concentration. The concentration of U(VI) in all experiments was determined by Arsenazo-III spectrophotometry at 650 nm. The removal efficiency (R%) was calculated by Eq. (1).

$$R\% = \frac{(C_0 - C_t)}{C_0} \times 100\% \qquad \text{Eq. (1)}$$

2. Characterization

PXRD spectra were obtained on a Bruker D8 diffractometer. FT-IR spectra were collected on a ThermoFisher Nicolet NEXUS 670 spectrophotometer. The morphologies of the four COFs were photographed on SEM (JEOL-7800F) and HRTEM-Mapping (HAADF-STEM, JEOL-2100F). The Solid-state ^{13}C nuclear magnetic resonance (NMR) spectra were performed using a Bruker AVANCE III 600 M spectrometer (600 MHz). The BET specific surface areas were obtained from Micromeritics ASAP 2020 apparatus. Elemental analysis (EA) was detected by an EA3000 analyzer (Euro Vector). Zeta Potential analysis (Malvern ZEN3690) was performed to study the surface charge properties of TpPa-N_x materials. XPS analysis were performed measured on using the Thermo Fisher ESCALAB 250Xi. The UV-visible diffused reflectance spectra (UV-vis DRS) were tested on a Shimadzu UV-2600 spectrophotometer with $BaSO_4$ as the background. The photoluminescence (PL) spectra were excited at 350 nm and the time-resolved photoluminescence (TRPL) spectra were determined on a HORIBA FluoroMax spectrophotometer. The electron spin resonance (ESR) spectra were detected by a Bruker MS 5000 instrument under visible light irradiation (300 W, lamp Au-Light). Free radicals •OH, e^-, $\bullet O_2^-$ and $^1O_2$ were detected by ESR using 5,5-dimethyl-1-pyrroline-N-oxide (DMPO) and 2,2,6,6-tetramethyl-4-piperidinol (TEMP) as trapping agents, respectively.

Transient photocurrent responses (*i-t*) and electrochemical impedance spectra (EIS) were carried out on a Shanghai Chenhua CHI 660E workstation with a standard three-electrode system. The TpPa-N_x materials were deposited on the ITO conductive

glass (1.0×1.0 cm^2) as the working electrode, Pt plate as the counter electrode and Ag/AgCl electrode as the reference electrode, as well as 0.25 M Na_2SO_4 solution was employed as the electrolyte. The Mott-Schottky (M-S) curves were measured at frequency of 1000, 1500, 2000 Hz, respectively, $E_{NHE} = E_{(Ag/AgCl)} + 0.197$ V.

3. DFT calculations

The structure information of TpPa-N_x materials was simulated by Materials Studio 2023 software. The electrostatic potentials (ESP) of TpPa-N_x materials were performed on Gaussian 09 software package using the B3LYP functional at the hybrid 6-31(d, p) method. The configuration geometry optimization for O_2 adsorption on TpPa-Nx materials was performed using the CASTEP module within Materials Studio 2023 software, employing plane-wave basis functions. The energy cutoff was set at 450 eV, with the energy convergence threshold of 1.0×10^{-6} eV at the gamma point. The vacuum layer between two neighboring layers of COFs was set to 15 Å, which was used to exclude the interaction between neighboring COFs layers. The adsorption energy (E_{ads}) of adsorbate on COFs can be calculated by using following equations by Eq. (2), where E_{total}, $E_{substrate}$, and $E_{adsorbate}$ are the total energies of the adsorption system, free adsorbate and substrate, respectively.

$$E_{ads} = E_{total} - (E_{substrate} + E_{adsorbate}) \quad \text{Eq. (2)}$$

4. Figures and tables

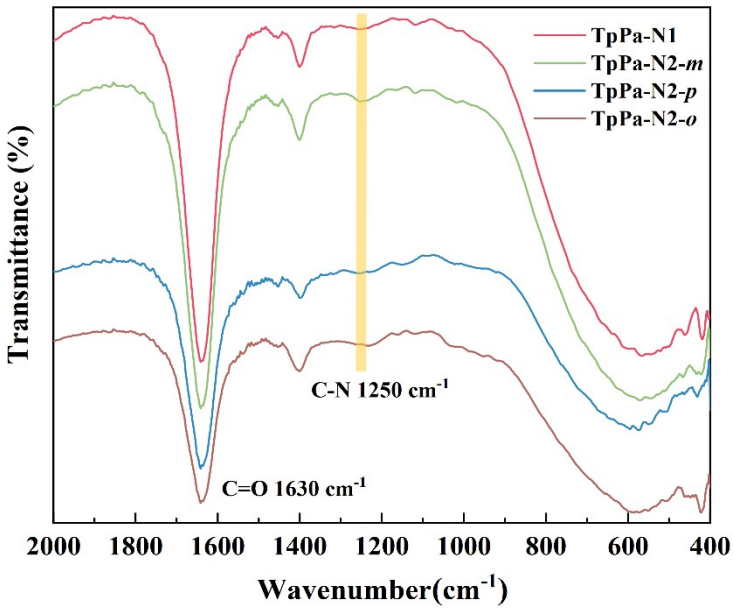

Fig. S1 The FT-IR spectra of TpPa-N1, TpPa-N2-*m*, TpPa-N2-*p* and TpPa-N2-*o*.

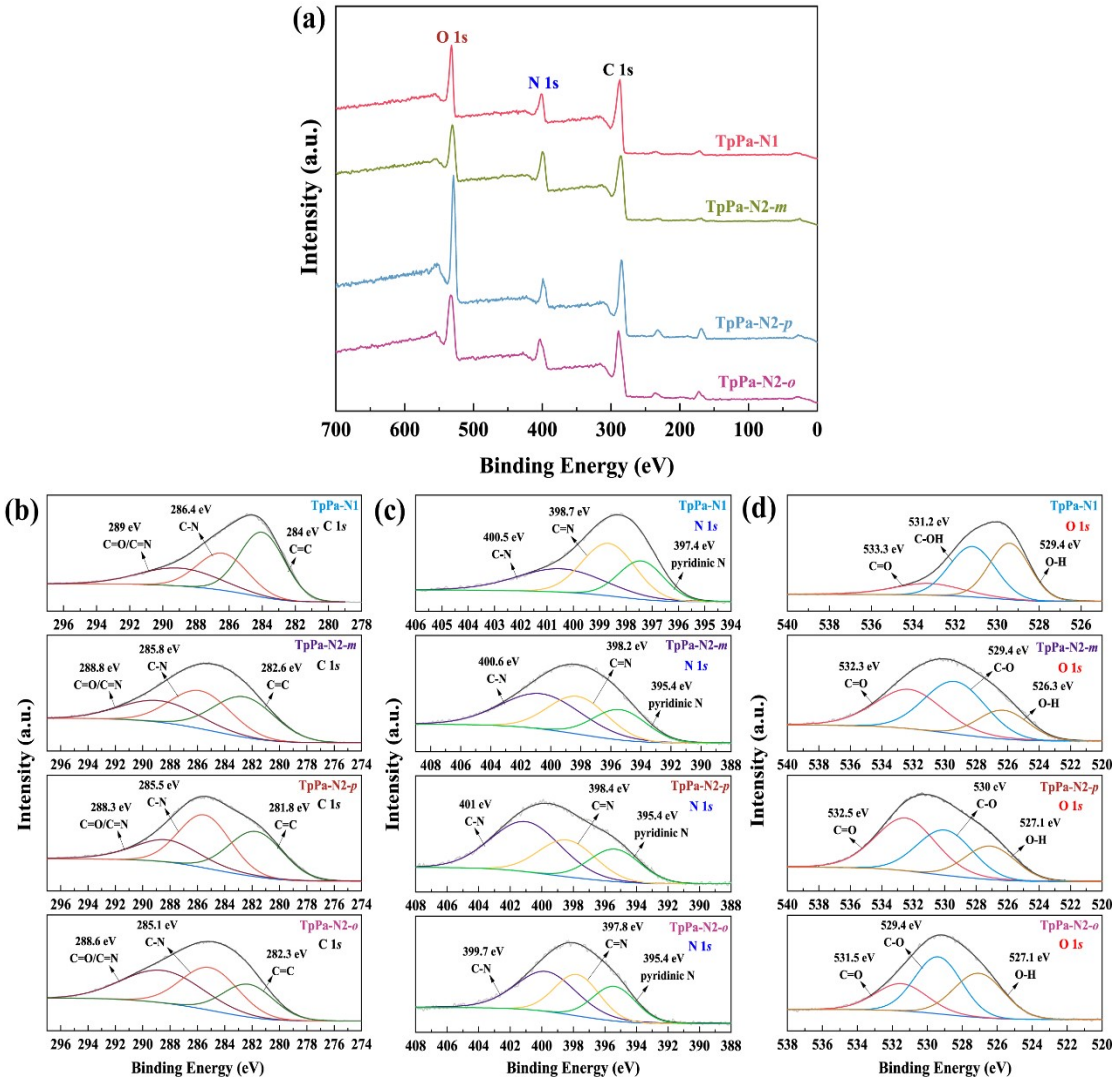

Fig. S2 (a) The XPS survey spectra, (b) high-resolution C 1s spectra, (c) N 1s spectra and (d) O 1s spectra of TpPa-N1, TpPa-N2-*m*, TpPa-N2-*p* and TpPa-N2-*o*.

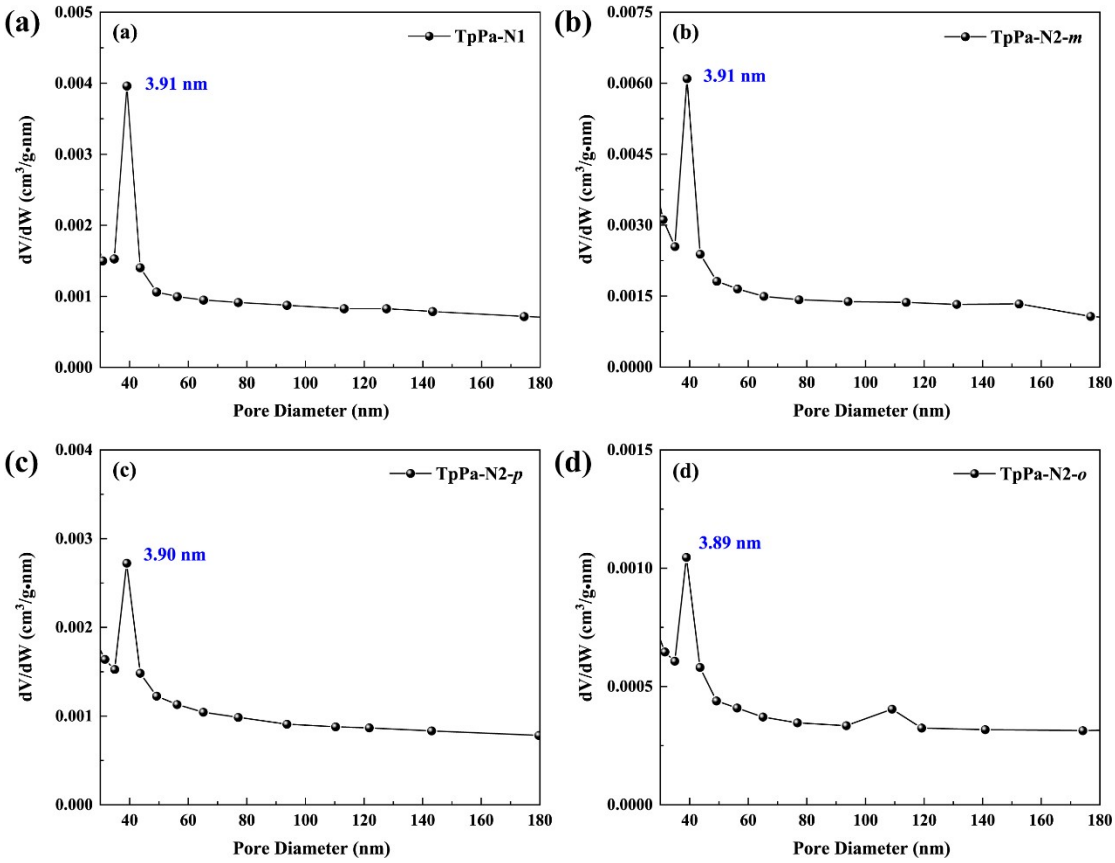

Fig. S3 The pore size distribution profiles of (a) TpPa-N1, (b) TpPa-N2-*m*, (c) TpPa-N2-*p* and (d) TpPa-N2-*o*.

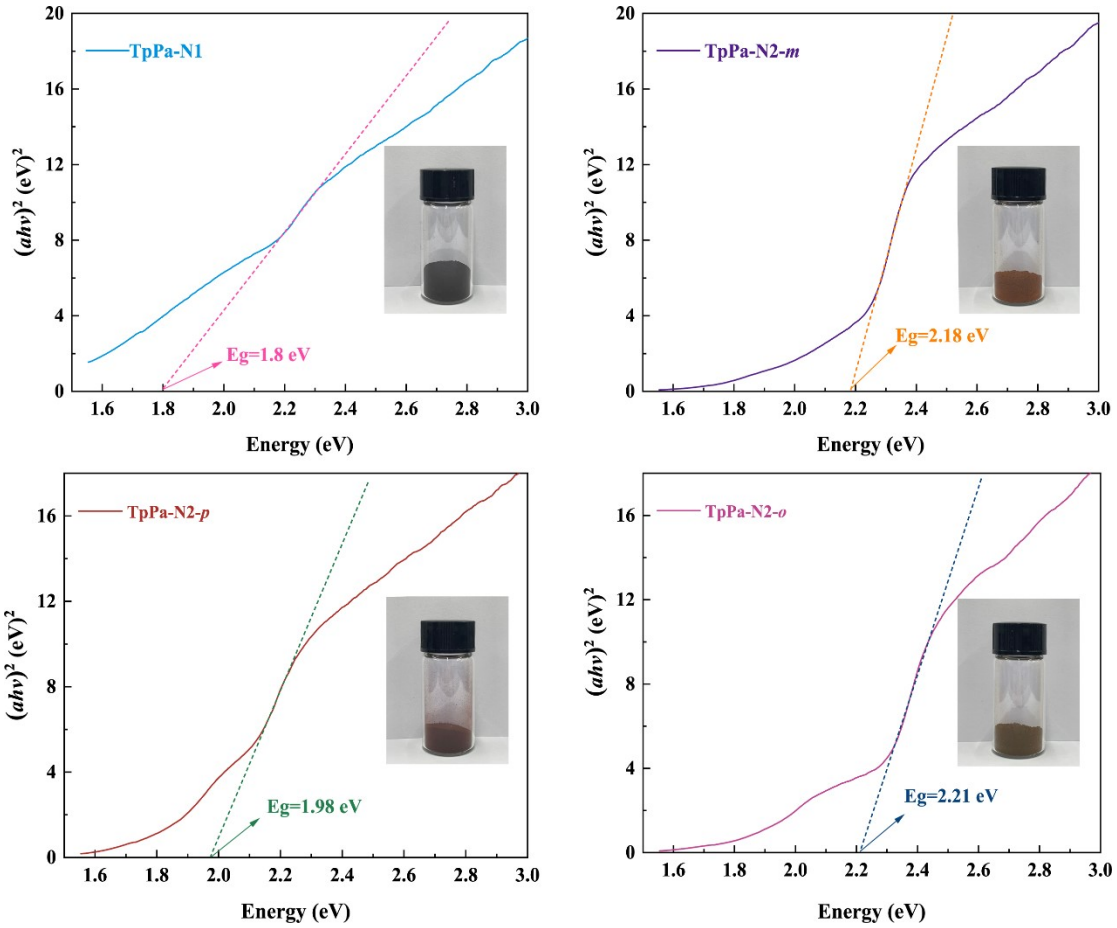

Fig. S4 Tauc plots of (a) TpPa-N1, (b) TpPa-N2-*m*, (c) TpPa-N2-*p* and (d) TpPa-N2-*o*.

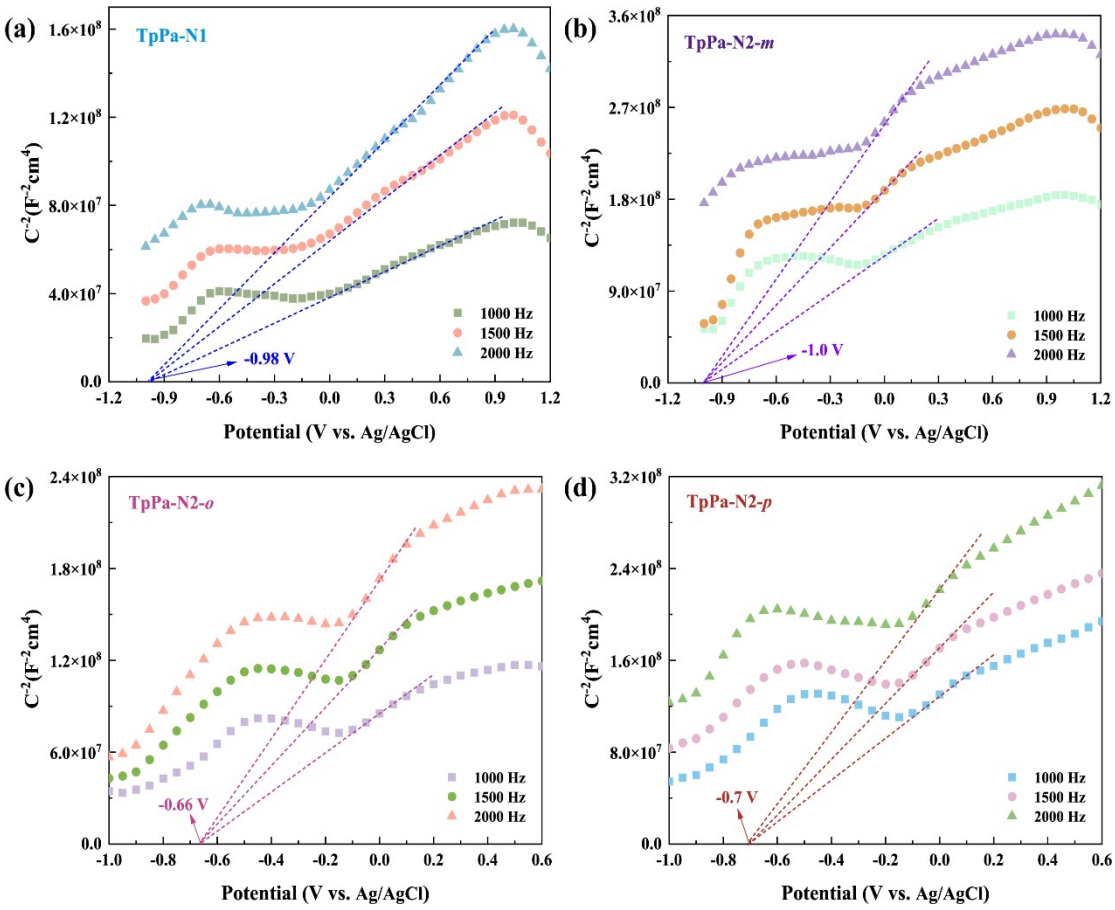

Fig. S5 The Mott-Schottky curves of (a) TpPa-N1, (b) TpPa-N2-*m*, (c) TpPa-N2-*p* and (d) TpPa-N2-*o*.

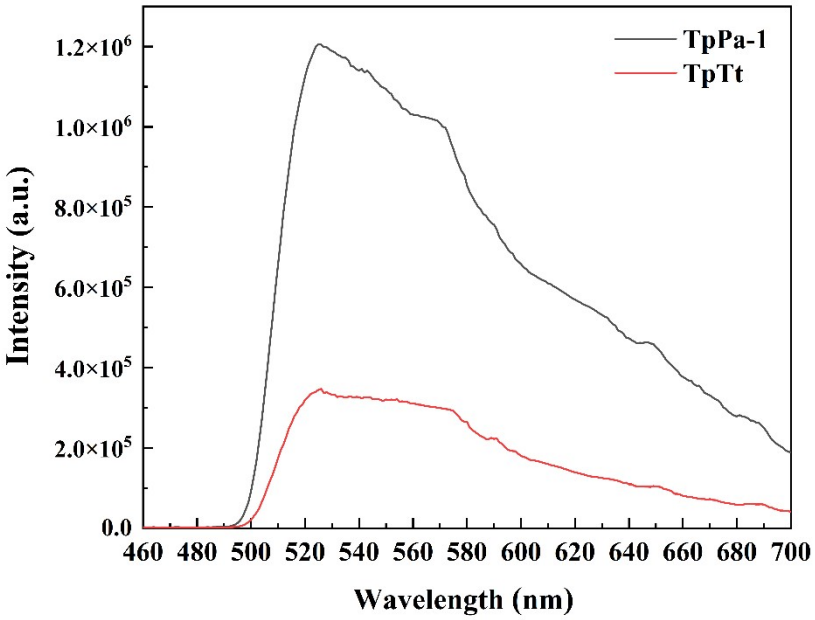

Fig. S6 The steady-state PL spectra of TpPa-1 and TpTt.

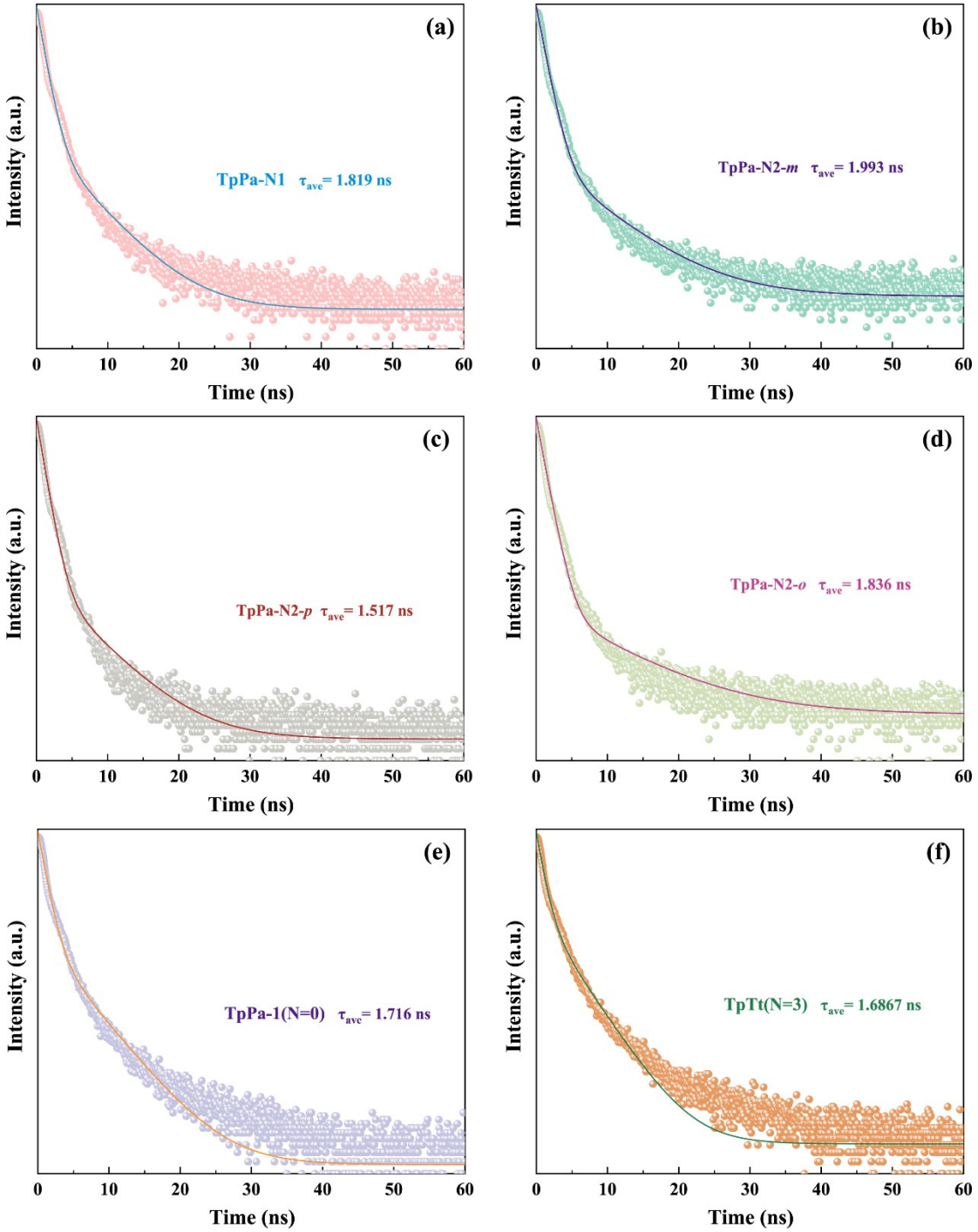

Fig. S7 The TRPL spectra of (a) TpPa-N1, (b) TpPa-N2-*m*, (c) TpPa-N2-*p*, (d) TpPa-N2-*o*, (e) TpPa-1 and (f) TpTt.

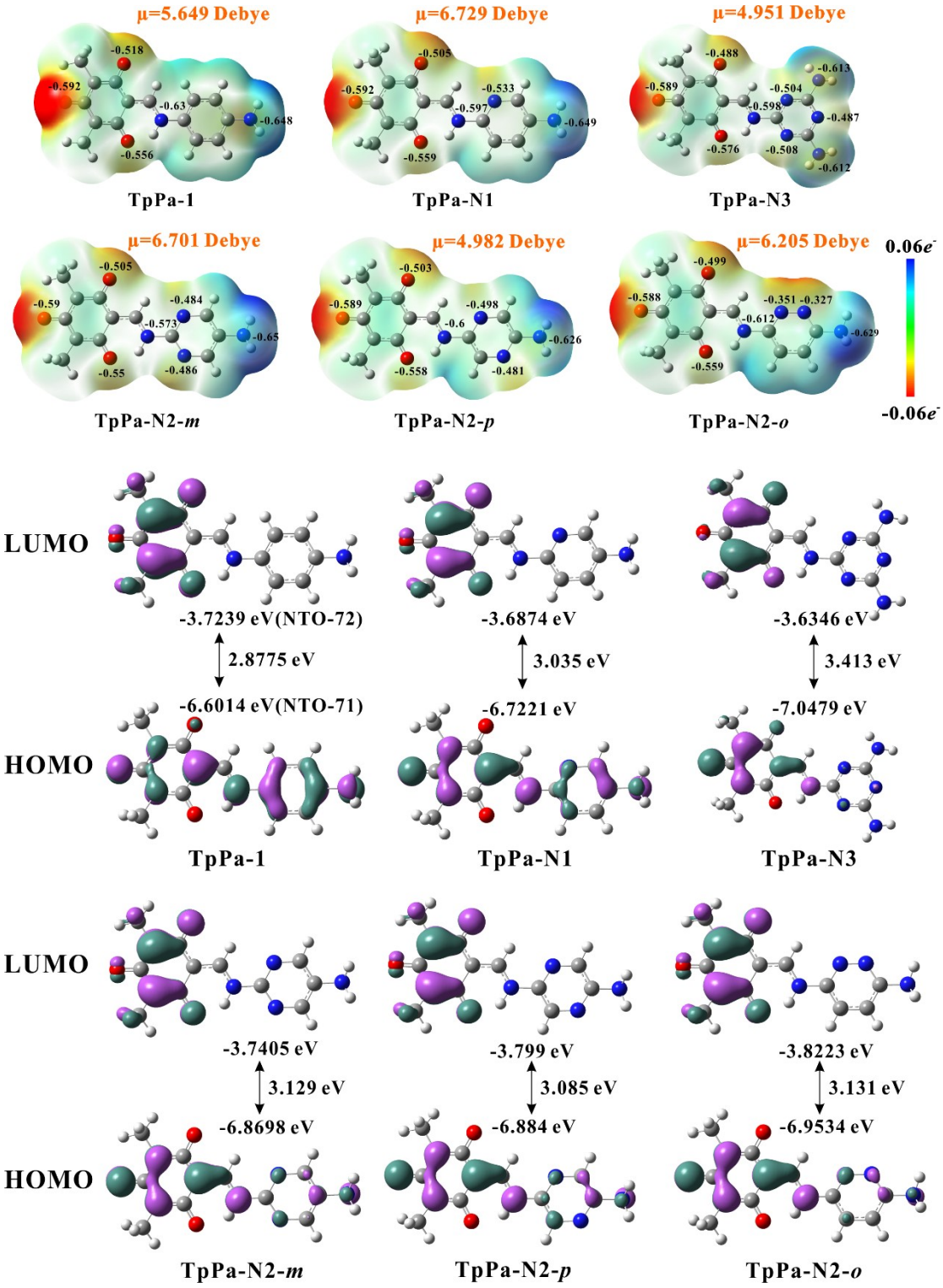

Fig. S8 ESP mapping, HOMO and LUMO orbitals of TpPa-N_x.

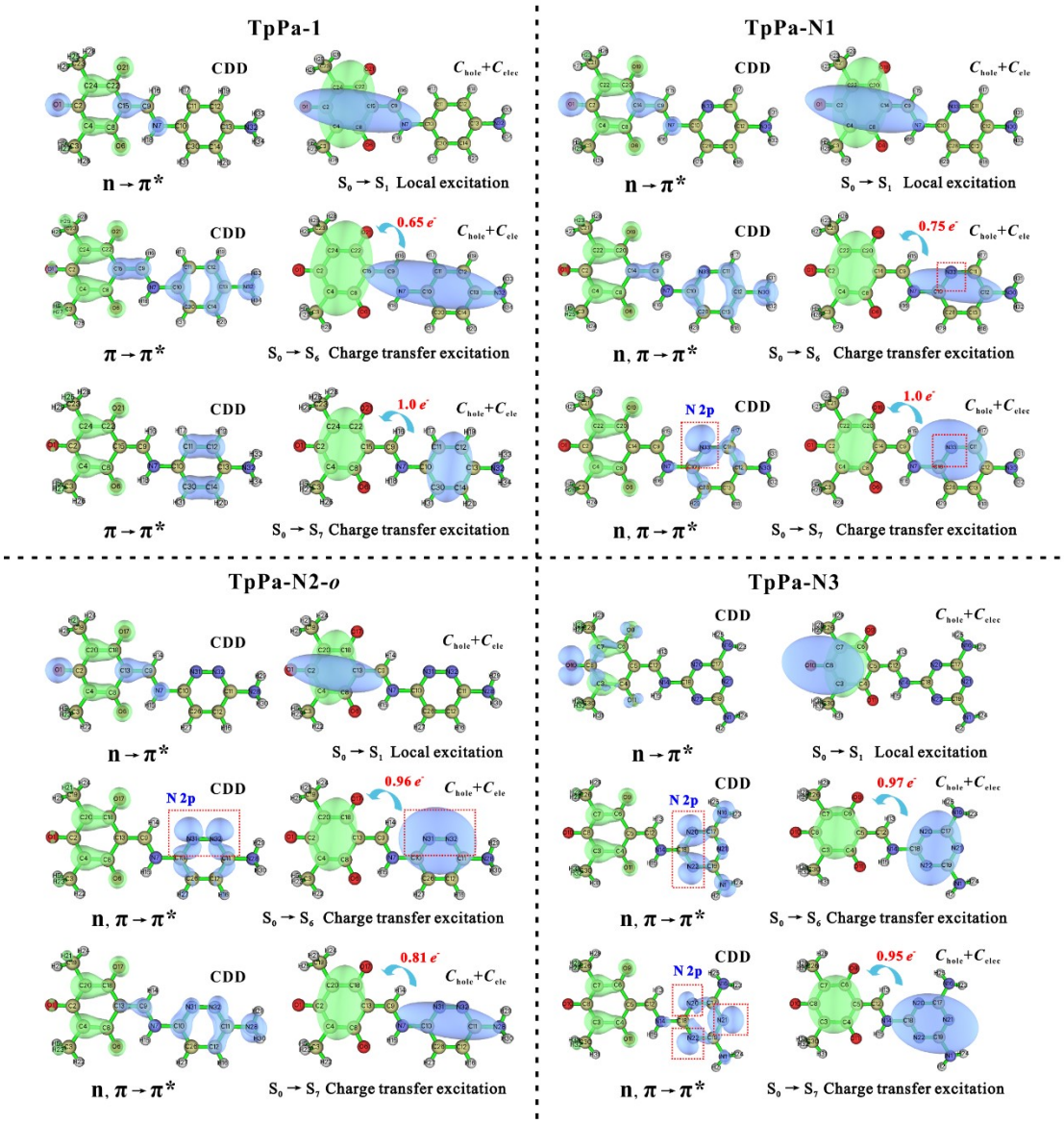

Fig. S9 Excited-state analysis of TpPa-N_x(x=0,1,2,3) (the blue area represents the hole distribution and the green area represents the electron distribution).

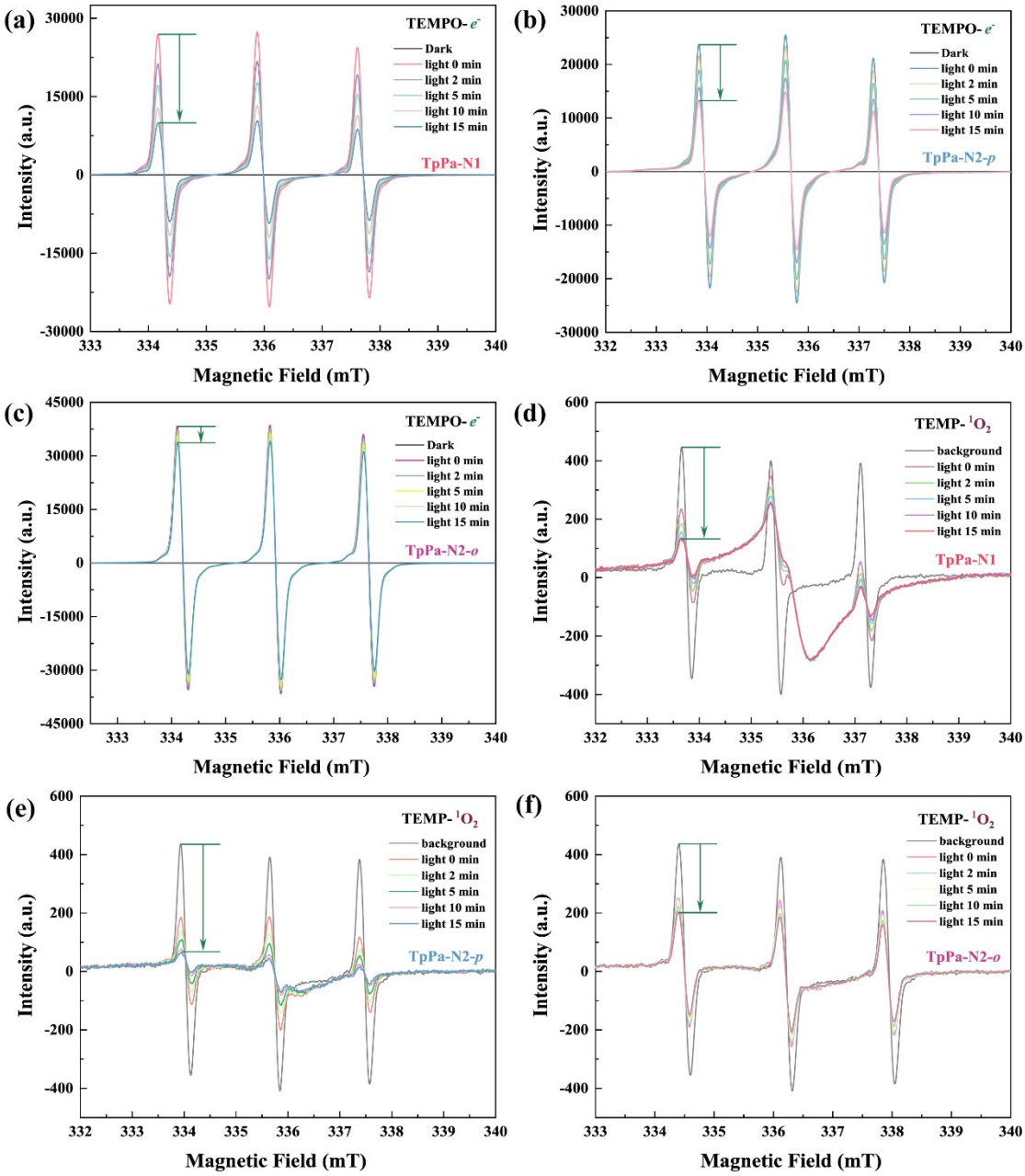

Fig. S10 EPR spectra of (a-c) TEMPO-e^- radical for TpPa-N1, TpPa-N2-*p* and TpPa-N2-*o*, and EPR spectra of (d-f) TEMP-$^1O_2$ radical for TpPa-N1, TpPa-N2-*p* and TpPa-N2-*o*.

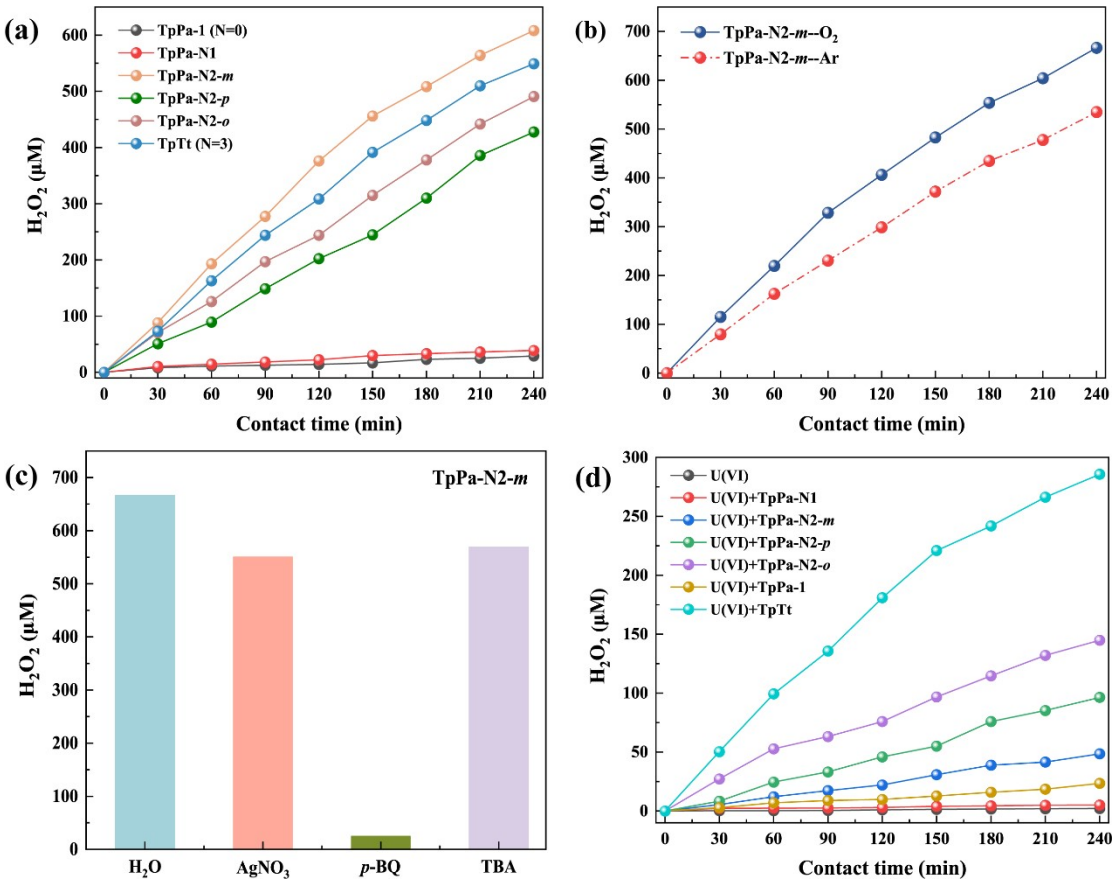

Fig. S11 (a) Photocatalytic H_2O_2 yields of TpPa-N_x(x=0,1,2,3) in pure water without any sacrificial agents (5 mg of catalyst, visible-light irradiation, Air), (b) the control experiment of photocatalytic H_2O_2 production by TpPa-N2-*m* under Ar and O_2 atmosphere, (c) the free radical trapping experiments during H_2O_2 production by TpPa-N2-*m* photocatalysis, (d) testing H_2O_2 generation in U(VI) solution (C_0=40 mg/L, visible-light irradiation, Air).

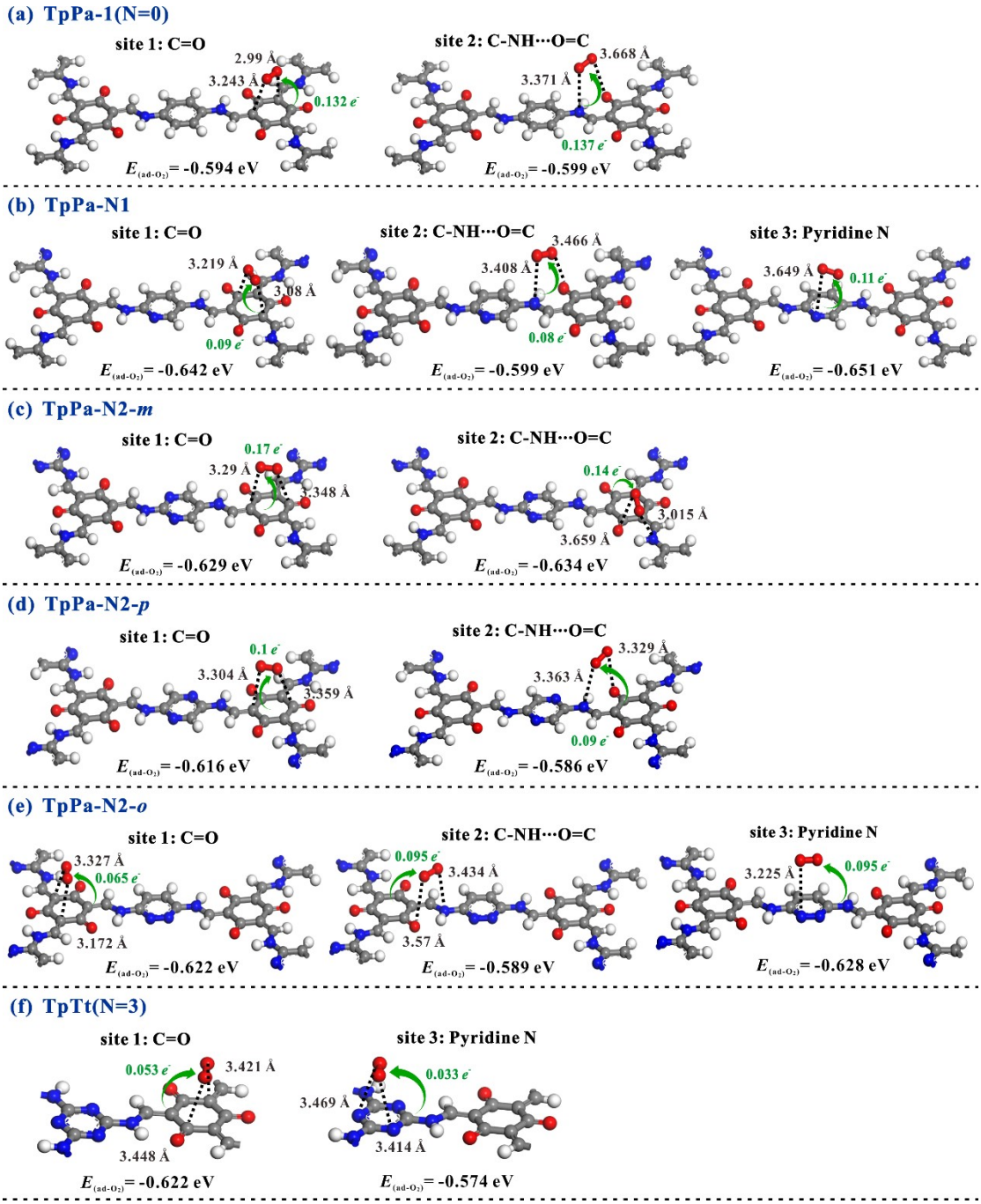

Fig. S12 (a-f) The adsorption configuration of O_2 molecule on TpPa-N_x(x=0,1,2,3).

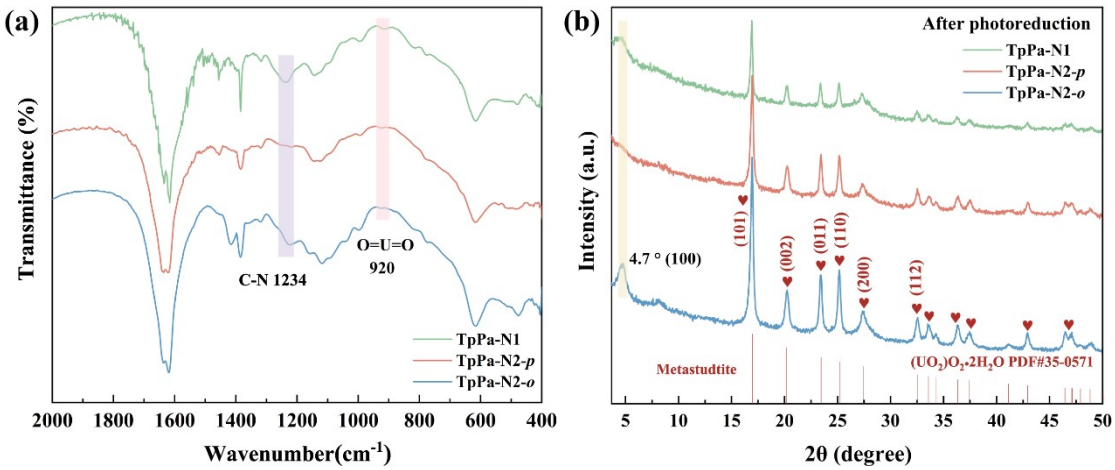

Fig. S13 (a) FT-IR and (b) XRD spectra of TpPa-N1, TpPa-N2-*p* and TpPa-N2-*o* after photoreduction.

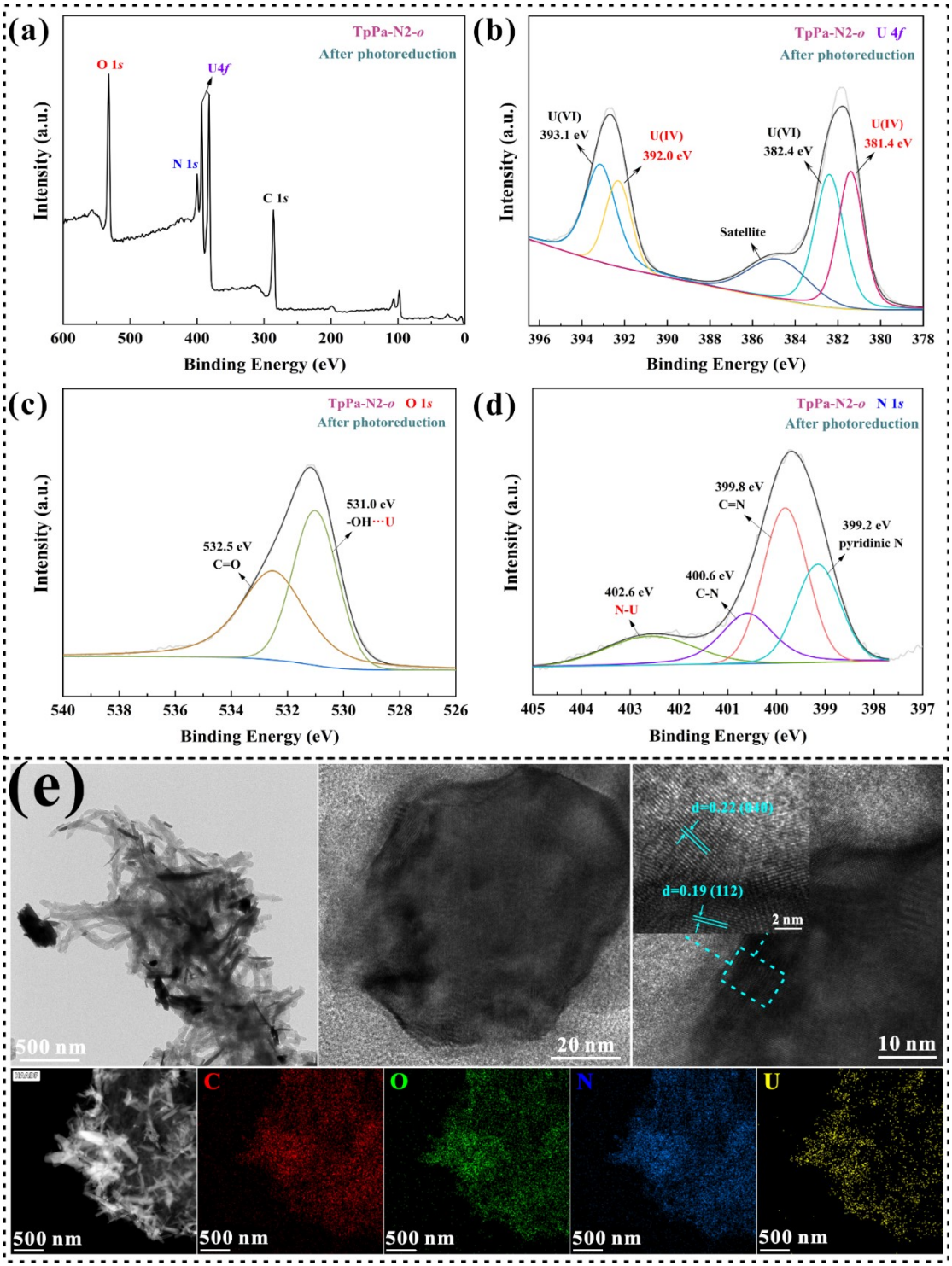

Fig. S14 XPS spectra of TpPa-N2-*o* after photoreduction: (a) survey spectrum, (b) U 4f, (c) O 1s, (d) N 1s spectrum and (e) HRTEM and elemental mapping images of TpPa-N2-*o* after photoreduction.

Table S1 The corresponding photocatalytic U(VI) reduction was given in the literature.

Photocatalysts	**Experimental conditions**	**Removal rates**	**Ref**
DAT-porphyrin	m/V=0.4 g/L, pH=6.0, 50 mg/L U(VI)	98.18%	[1]
TFA-TAT-COF-Q	m/V=0.125 g/L, 50 mg/L U(VI), pH=5.0	97%	[2]
B-TiO_2@Co_2P-500	m/V=0.25 g/L, 8 mg/L U(VI), pH=5.0	98%	[3]
g-C_3N_4@$ZnIn_2S_4$	m/V= 0.1 g/L, 50 mg/L U(VI), pH=7.0	97.4%	[4]
CdS-Rod	m/V= 0.1 g/L, 30 mg/L U(VI), pH=5.0	99%	[5]
PEO-COF	m/V=0.2 g/L, 400 mg/L U(VI), pH=5.0	100%	[6]
TpPa-N2-*m*	m/V=0.06 g/L, 25 mg/L U(VI), pH=6.0, 3 mL CH_3OH	94.4%	**This work**

References

[1] P. Wu, X. Yin, Y. Zhao, F. Li, Y. Yang, N. Liu, J. Liao, T. Lan, Porphyrin-based hydrogen-bonded organic framework for visible light driven photocatalytic removal of U(VI) from real low-level radioactive wastewater, J Hazard Mater, 459 (2023) 132179.

[2] C. Liu, Y. Wang, Z. Dong, Z. Zhang, X. Cao, Y. Zhai, Y. Liu, Covalent organic frameworks for enhanced photocatalytic extraction of uranium via the modulation of charge transfer pathways, Chemical Engineering Journal, 514 (2025) 163078.

[3] F. Zhang, H. Dong, Y. Li, D. Fu, L. Yang, Y. Shang, Q. Li, Y. Shao, W. Gang, T. Ding, T. Chen, W. Zhu, In Situ Metal-Oxygen-Hydrogen Modified B-TiO_2@Co_2P-X S-Scheme Heterojunction Effectively Enhanced Charge Separation for Photo-assisted Uranium Reduction, Adv Sci (Weinh), 11 (2024) e2305439.

[4] Z. Zheng, X. Wang, Z. Ye, R. jin, H. Qiu, J. Chen, Y. Wang, Z. Dong, Z. Zhang, Y. Liu, In situ growth $ZnIn_2S_4$ nanosheets on g-C_3N_4 nanorods with boosted charge transfer for high-efficient photocatalysis removal of U(VI), Separation and Purification Technology, 364 (2025) 132271.

[5] Y. Quan, S. Lu, Q. Wang, H. Wang, E. Hu, X. Wang, J. Bao, X. Sun, K. Li, P. Ning, Unveiling shape-dependent intrinsic activity of cadmium sulfide (CdS) for photocatalytic uranium(VI) reduction, Chemical Engineering Journal, 506 (2025) 160199.

[6] X. X. Wang, C. R. Zhang, R. X. Bi, Z. H. Peng, H. X. He, R. Zhang, A. M. Song, J. X. Qi, X. J. Chen, X. Liu, Y. J. Cai, R. P. Liang, J.-D. Qiu, Tuning local charge polarization of covalent organic frameworks for enhanced photocatalytic uranium (VI) reduction, Chemical Engineering Journal, 499 (2024) 156483.